Theoret. chim. Acta (Berl.) 22, 45—60 (1971)

Theory of Magnetism Close to the $^5T_2 - {}^1A_1$ Crossover in Iron(II) Complexes

II. Full Configuration Interaction Calculation in a Cubic Field

E. KÖNIG and S. KREMER

Institut für Physikalische Chemie II, University of Erlangen-Nürnberg, 8520 Erlangen, Germany

Received February 17, 1971

On the basis of the eigenvalues and the eigenvectors resulting from the diagonalization of the complete ligand field, Coulomb interaction, and spin-orbit coupling matrices, the magnetic susceptibility has been calculated for the d^6 configuration in a field of octahedral symmetry. The magnetic moment values μ_{eff} are presented as function of temperature and 10 Dq for a fixed set of values of the Racah parameters B, C and the spin-orbit coupling constant ζ. The region of the $^5T_2$—$^1A_1$ crossover is considered in detail and the application to relevant experimental data is discussed.

Die vollständigen Matrizen, die das Ligandenfeld, die Coulombwechselwirkung und die Spin-Bahn-Kopplung enthalten, wurden aufgestellt und die durch ihre Diagonalisierung erhaltenen Eigenwerte und Eigenvektoren wurden benutzt, um die magnetische Suszeptibilität für die Konfiguration d^6 in einem Feld oktaedrischer Symmetrie zu berechnen. Das magnetische Moment μ_{eff} wird als Funktion der Temperatur und 10 Dq für feste Werte der Racah-Parameter B, C und der Spin-Bahn-Kopplungskonstante ζ angegeben. Der Bereich des $^5T_2 - {}^1A_1$-Überschneidungspunktes wird eingehend betrachtet und die Anwendung auf geeignete experimentelle Daten wird diskutiert.

En utilisant les valeurs et les vecteurs propres des matrices complètes: champ des ligands, interaction coulombienne et couplage spin-orbite, la susceptibilité magnétique a été calculée pour la configuration d^6 dans un champ de symétrie octaédrique. Les valeurs du moment magnétique μ_{eff} sont présentées comme fonction de la température et de 10 Dq pour une valeur donnée des paramètres B et C de Racah et de la constante de couplage spin-orbite. La zone du croisement $^5T_2 - {}^1A_1$ est examinée en détail et les données expérimentales correspondantes sont discutées.

Introduction

In a previous paper [1] we have briefly reviewed the magnetic properties of iron(II) complexes in which a $^5T_2 - {}^1A_1$ crossover is either established or supposedly involved. An attempt has been made to develop a semi-empirical theory suitable to reproduce the experimental magnetic data of such systems. It was shown that a modification of the two-level scheme including at least an axial field distortion and taking account of permanently paramagnetic material was needed. In all compounds studied in some detail, the axial field splitting of the $^5T_2$ term is such as to produce a low lying orbital singlet (i.e. $^5B_2$, if the distortion is tetragonal). This is equivalent to the axial field parameter δ being negative and varying, in actual compounds, between about -200 and $-1000\ cm^{-1}$.

Based on a comparison of calculated and experimental magnetic data it was demonstrated that the energy separation ε between the centers of gravity of the $^5T_2$

and $^1A_1$ terms is strongly temperature-dependent. This result is consistent with the decrease of the Fe-ligand bond distance which is expected on change of the groundstate from $^5T_2(t_2^4e^2)$ to $^1A_1(t_2^6)$ [2]. In one case, the change of the Fe-ligand bond length has been demonstrated directly by X-ray structure methods [3]. Specific values for $\varepsilon = \varepsilon(T)$ were determined in two systems, *viz.* $[Fe(mephen)_3](ClO_4)_2$ and $[Fe(mephen)_3](BF_4)_2$ where mephen = 2-methyl-1,10-phenanthroline [4]. In these compounds, the parameter δ was estimated from the temperature dependence of the quadrupole splitting in the ^{57}Fe Mössbauer spectra [5]. Additional results on systems of related interest will be published separately [6].

In the present study, the magnetic properties of a d^6 electron system will be calculated by means of ligand field theory. We are interested particularly in the region close to the $^5T_2 - {}^1A_1$ crossover, in the mixing effects of excited terms on the magnetic susceptibility and in the temperature dependence of the ligand field splitting parameter 10 Dq and of the $^5T_2 - {}^1A_1$ energy separation ε. Therefore, full configuration and spin-orbit interaction will be included. Since, in this investigation, accurate reproduction of experimental data is considered only on a second priority basis, we will disregard axial and lower symmetry distortions and assume, in what follows, a cubic field to be present.

Octahedral Ligand Field and Interelectronic Repulsion Matrices and Resulting Eigenvectors

The combined ligand field and interelectronic repulsion matrices for a d^6 transition metal ion in a field of octahedral symmetry were derived by Tanabe and Sugano [7, 8]. These authors also performed detailed numerical calculations on the d^6 Co^{3+} ion. In Fig. 1 we present the results of similar calculations on the low lying excited states of the Fe^{2+} ion. In analogy to the Tanabe-Sugano diagrams [7, 8], E/B is plotted versus Δ/B where E is the energy relative to the ground state and $\Delta = 10$ Dq the octahedral ligand field splitting parameter. Free ion values of the Racah interelectronic repulsion parameters (*viz.* $B = 917\ cm^{-1}$, $C = 4040\ cm^{-1}$) were used. The crossover between the groundstates $^5T_2$ and $^1A_1$ occurs, within this approximation, at $10\ Dq = \Pi \sim 17{,}006.8\ cm^{-1}$. Without configuration interaction, the $^5T_2 - {}^1A_1$ energy separation is determined according to

$$\varepsilon = 20\ Dq - 5B - 8C \tag{1}$$

whereas if non-diagonal matrix elements are approximately accounted for [9],

$$\varepsilon = 20\ Dq - 5B - 8C + \frac{120B^2}{10\ Dq}. \tag{2}$$

It should be observed that the value of Π at the crossover as determined from Eq. (1) or Eq. (2) with $\varepsilon = 0$ is largely in error. Thus using the values of B and C listed above, Eq. (1) results in $\Pi = 18{,}452.5\ cm^{-1}$, whereas the quadratic Eq. (2) gives the value $\Pi = 15{,}114.4\ cm^{-1}$ which is no better. Both equations provide, therefore, only very crude estimates of the crossover energy Π.

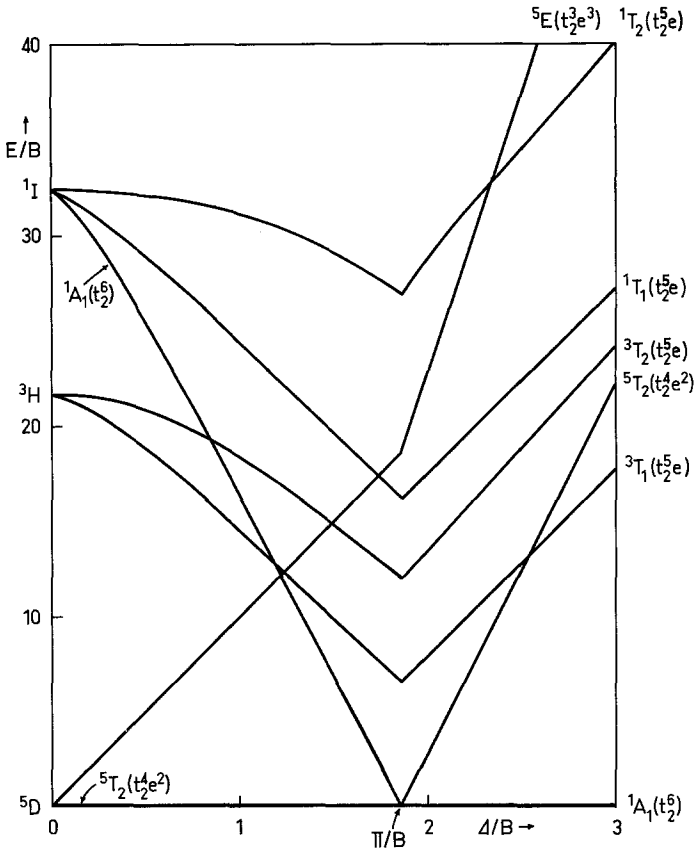

Fig. 1. Energy versus $\Delta = 10$ Dq for the lowest states of the Fe^{2+} ion in a ligand field of octahedral symmetry (in units of B; $B = 917\ cm^{-1}$, $C = 4040\ cm^{-1}$)

The wavefunctions of the three lowest terms depicted in Fig. 1, i.e. $^5T_2$, $^1A_1$, and $^3T_1$, may be written, if configuration interaction is included, as

$$
\begin{aligned}
|^5T_2\rangle &= |t_2^4\, e^2\rangle \\
|^1A_1\rangle &= \alpha|t_2^6\rangle + \beta|t_2^4(^1E)\, e^2(^1E)\rangle + \gamma|t_2^4(^1A_1)\, e^2(^1A_1)\rangle \\
&\quad + \delta|t_2^3(^2E)\, e^3\rangle + \varepsilon|t_2^2\, e^4\rangle \\
|^3T_1\rangle &= \zeta|t_2^5\, e\rangle + \eta|t_2^4(^1T_2)\, e^2(^3A_2)\rangle + \theta|t_2^4(^3T_1)\, e^2(E)\rangle \\
&\quad + \kappa|t_2^4(^3T_1)\, e^2(^1A_1)\rangle + \lambda|t_2^3(^2T_2)\, e^3\rangle + \mu|t_2^3(^2T_1)\, e^3\rangle \\
&\quad + \nu|t_2^2\, e^4\rangle
\end{aligned}
\tag{3}
$$

where $\alpha, \beta, \ldots, \nu$ are coefficients dependent on 10 Dq. Since we are interested in the properties close to the crossover, we determined the eigenvectors of Eq. (3) by solving the ligand field plus interelectronic repulsion matrices of Fe^{2+} for the

particular value 10 Dq = Π:

$$
\begin{aligned}
|^5T_2\rangle &= |t_2^4\, e^2\rangle \\
|^1A_1\rangle &= 0.981\,|t_2^6\rangle + 0.029\,|t_2^4(^1E)\, e^2(^1E)\rangle - 0.188\,|t_2^4(^1A_1)\, e^2(^1A_1)\rangle \\
&\quad + 0.029\,|t_2^3(^2E)\, e^3\rangle + 0.029\,|t_2^2\, e^4\rangle \\
|^3T_1\rangle &= 0.981\,|t_2^5\, e\rangle - 0.041\,|t_2^4(^1T_2)\, e^2(^3A_2)\rangle \\
&\quad - 0.121\,|t_2^4(^3T_1)\, e^2(^1E)\rangle + 0.084\,|t_2^4(^3T_1)\, e^2(^1A_1)\rangle \\
&\quad + 0.009\,|t_2^3(^2T_2)\, e^3\rangle + 0.022\,|t_2^3(^2T_1)\, e^3\rangle + 0.120\,|t_2^2\, e^4\rangle\,.
\end{aligned}
\tag{4}
$$

Spin-Orbit Interaction

The degeneracy of the various terms resulting from the d^6 electron configuration is partially removed by spin-orbit interaction

$$\mathscr{H}_{so} = \kappa\zeta_{3d}\, \boldsymbol{l}_i \cdot \boldsymbol{s}_i\,, \tag{5}$$

where ζ_{3d} is the $3d$-electron spin-orbit coupling constant and κ the Stevens' orbital reduction factor. In the three terms of lowest energy the effect of the interaction according to Eq. (5) is, to first order, to separate the $^5T_2$ and $^3T_1$ terms into three levels each with energies of 3λ, λ, -2λ and λ, $-\lambda$, -2λ, respectively. To higher order the splitting by the spin-orbit interaction is according to

$$
\begin{aligned}
{}^5T_2 &\rightarrow \Gamma_1 + \Gamma_3 + 2\Gamma_4 + 2\Gamma_5 \\
{}^3T_1 &\rightarrow \Gamma_1 + \Gamma_3 + \Gamma_4 + \Gamma_5
\end{aligned}
\tag{6}
$$

whereas $^1A_1 \rightarrow \Gamma_1$ and is not split, *viz.* Fig. 2. Here it is $\lambda = \pm\zeta_{3d}/2S$ and we use the Bethe notation for levels resulting from spin-orbit interaction. In ligand fields close to 10 Dq = Π, the levels originating in the $^5T_2$ and $^1A_1$ states are within kT and the levels from the $^3T_1$ are within $\sim 6000\ \mathrm{cm}^{-1}$ of the groundstate. This gives rise to a noticeable amount of spin-orbit mixing between levels belonging to the same irreducible representation Γ_j. In addition, the wavefunctions Eq. (4) demonstrate that there is a significant mixing with higher energy levels via configuration interaction. Therefore, it is desirable to consider the complete matrices containing the ligand field, interelectronic repulsion, and spin-orbit interactions within the d^6 configuration.

The complete problem is represented by the Hamiltonian

$$\mathscr{H} = \sum_{i=1}^{6} \left\{ -\frac{\hbar^2}{2m} \boldsymbol{V}_i^2 - \frac{Z\, e^2}{r_i} + \kappa\zeta_{3d}\, \boldsymbol{l}_i \cdot \boldsymbol{s}_i \right\} + \sum_{i>j}^{6} \frac{e^2}{r_{ij}} + V_{O_h}\,. \tag{7}$$

The required matrices may be easily constructed, within the strong-field approximation, following the procedures outlined by Griffith [10]. The relevant wavefunctions of the various terms $^{2S+1}\Gamma$ which originate in the strong-field configurations $t_{2g}^m\, e_g^n$ may be written thus

$$|t_{2g}^m(S_1\,\Gamma_1)\, e_g^n(S_2\,\Gamma_2)\, S\,\Gamma\, M\,\gamma\rangle\,.$$

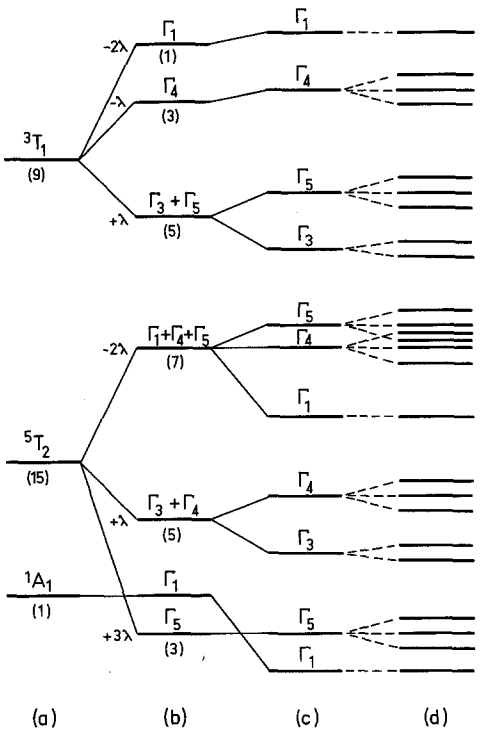

Fig. 2. Schematic energy level splitting for the lowest states ($^5T_2$, $^1A_1$, and $^3T_1$) of a d^6 ion in O_h symmetry (not to scale): a) octahedral ligand field only; b) first-order spin-orbit interaction; c) higher order spin-orbit interaction; d) effect of an external magnetic field. It should be observed that λ is negative

These functions which we will abbreviate as $|\alpha S\Gamma M\gamma\rangle$ were obtained from the component strong-field wavefunctions, *viz.* $|t_{2g}^m S_1 \Gamma_1\rangle$ and $|e_g^n S_2 \Gamma_2\rangle$, using vector coupling relations [10]. In the above kets, M is used instead of M_S, γ denotes one of the components of the irreducible representation Γ, and α is used to distinguish states belonging to the same $S\Gamma$. The spin and orbital parts are then coupled according to

$$\Gamma \times D^{(S)} = \sum_T c_T \Gamma_T$$

to yield "total" states transforming as Γ_T of O_h,

$$|\alpha S\Gamma\beta\Gamma_T\gamma_T\rangle = \sum_{M\gamma} \langle S\Gamma M\gamma|\beta\Gamma_T\gamma_T\rangle|\alpha S\Gamma M\gamma\rangle\,. \tag{8}$$

In Eq. (8), the quantum number β has been introduced to distinguish states with the same $\alpha S\Gamma$ and the same $\Gamma_T\gamma_T$ and $D^{(S)}$ is the representation of spin S in the octahedral group. Also, in what follows, we will use the Mulliken notation (*viz.* A_1, A_2, E, T_1, T_2) to label irreducible representations specifying orbital states and the Bethe notation (*viz.* Γ_i, $i = 1, 2, \ldots, 5$) to label total states Γ_T. The wavefunctions $|\alpha S\Gamma\beta\Gamma_T\gamma_T\rangle$, cf. Eq. (8), have then been employed to calculate matrix elements of

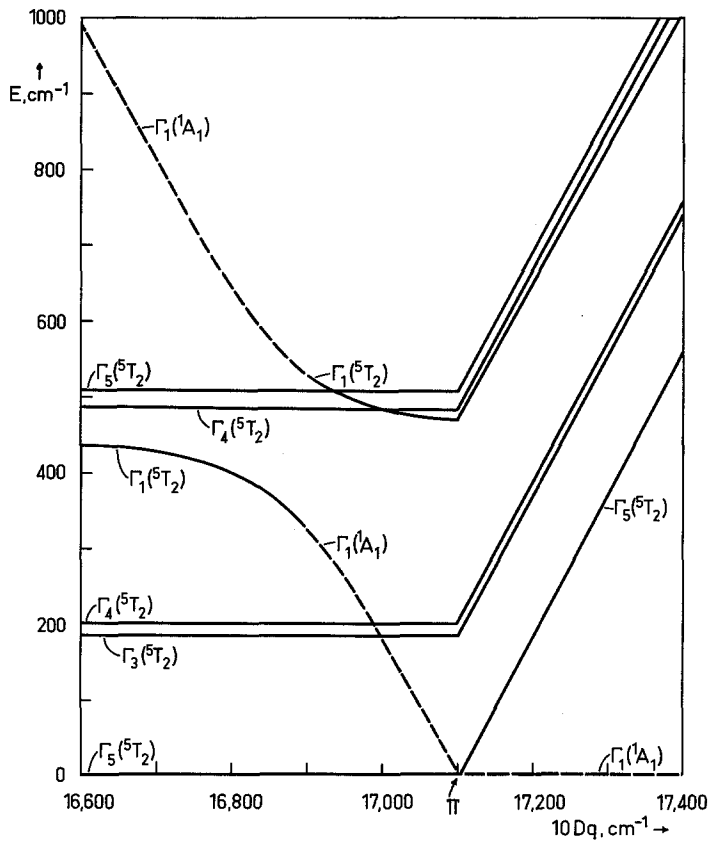

Fig. 3. Central region of the complete octahedral ligand field and spin-orbit interaction diagram. The crossover occurs at 10 Dq = Π = 17,100 cm^{-1}. Broken line: $\Gamma_1[^1A_1(t_2^6)]$ level; full lines: spin-orbit components of the $^5T_2(t_2^4e^2)$ term

the spin-orbit coupling operator $\sum_i \kappa\zeta \boldsymbol{l}_i \cdot \boldsymbol{s}_i$. The matrix elements of the inter-electronic repulsion and of the ligand field were taken from Griffith [10].

We diagonalized the resulting 91 × 91 matrix of the exact secular problem [11] in order to obtain the eigenvalues and eigenvectors of the Hamiltonian Eq. (7). Fig. 3 illustrates the results with respect to the lowest energy levels close to 10 Dq = Π if the free ion values of B, C and $\zeta = 420$ cm^{-1} are employed. This Figure shows the modifications to the center of Fig. 1 which arise due to spin-orbit coupling. It is seen that, at 10 Dq = 16,900 cm^{-1}, the levels $\Gamma_1[^1A_1(t_2^6)]$ and $\Gamma_1[^5T_2(t_2^4e^2)]$ change their labels as a consequence of their mutual interaction and the non-crossing rule. The crossover occurs approximately at 10 Dq = Π = 17,100 cm^{-1} since, at this value of 10 Dq, the energy of $\Gamma_1(^1A_1)$ is only 1.44 cm^{-1} above $\Gamma_5(^5T_2)$.

The spin-orbit matrices for the equivalent d^4 system were derived previously by Schroeder [12] employing tensor operator methods. We checked via computer diagonalization that the combination of corresponding d^6 spin-orbit matrices

with the d^6 Tanabe-Sugano matrices [7, 8] is equivalent to the matrices employed by us.

The functions $|\alpha S\Gamma\beta\Gamma_T\gamma_T\rangle$ introduced above are mixed again on diagonalization of the resulting spin-orbit matrices provided they belong to the same $\Gamma_T\gamma_T$. Therefore, the eigenvectors diagonalizing the complete Hamiltonian Eq. (7) may be written

$$|\tilde{\beta}\Gamma_T\gamma_T\rangle = \sum_{j=1}^{N} C_j|\alpha S\Gamma\beta\Gamma_T\gamma_T\rangle \tag{9}$$

where the summation extends over all kets $|\alpha S\Gamma\beta\Gamma_T\gamma_T\rangle$ within the same $\Gamma_T\gamma_T$ which are characterized by different $\alpha S\Gamma\beta \equiv j$. In the table, we list the irreducible representations Γ_T together with their dimensions N which are identical to the number of the eigenvectors Eq. (9).

Table

Γ_T	Γ_1	Γ_2	Γ_3	Γ_4	Γ_5
N	14	8	19	23	27

Detailed expressions for the eigenvectors Eq. (9) resulting from the lowest energy terms $^5T_2$, $^1A_1$, and $^3T_1$ at $10\,\mathrm{Dq} = \Pi = 17{,}100\,\mathrm{cm}^{-1}$ are listed in Appendix I.

Effect of an External Magnetic Field and the Calculation of Magnetic Susceptibility

The application of an external magnetic field may be represented by the operator

$$\mathscr{H}_m = \hbar^{-1}\beta \sum_{i=1}^{6} (\kappa \boldsymbol{l}_i + 2\boldsymbol{s}_i)\boldsymbol{H} \tag{10}$$

where β is the Bohr magneton and $\boldsymbol{H}$ the magnetic field strength which may be taken, in a ligand field of octahedral symmetry, in the z direction. $\mathscr{H}_m$ operates on the eigenvectors $|\beta\Gamma_T\gamma_T\rangle$, cf. Eq. (9). Since the remaining degeneracy of the system will be lifted by the action of the magnetic field, states distinguished by different γ_T have to be considered separately. There are altogether 210 different kets $|\beta\Gamma_T\gamma_T\rangle$ corresponding to the dimensions N and the degeneracies of the representations Γ_T (*viz.* the table). The application of $\mathscr{H}_m$ on the $|\beta\Gamma_T\gamma_T\rangle$ thus generates the matrix elements

$$\langle\beta\Gamma_T\gamma_T|\sum_i \beta(\kappa l_{iz} + 2s_{iz})H_z|\beta'\Gamma'_T\gamma'_T\rangle \tag{11}$$

(in units of $\hbar$) which form a 210×210 matrix. A conventional calculation of the Zeeman energy would require the solution, at least in an approximate form, of the secular problem corresponding to the matrix Eq. (11). Since we are interested only in the magnetic susceptibility, certain simplifications are possible.

In general, the magnetic field removes the j_n-fold degeneracy of a level E_n. If the sublevels are specified by a suffix m, the energy of any magnetic level E_{nm} may be expanded as a power series in the applied magnetic field H,

$$E_{nm} = E_n^{(0)} + E_{nm}^{(1)} H + E_{nm}^{(2)} H^2 + \cdots . \tag{12}$$

The molar magnetic susceptibility is then obtained by taking the statistical average over all the energy levels resulting from the application of Eq. (10) using a Boltzmann distribution [13],

$$\chi_m = N \frac{\sum\limits_{n,m} \left(\frac{[E_{nm}^{(1)}]^2}{kT} - 2E_{nm}^{(2)} \right) e^{-E_n^{(0)}/kT}}{\sum\limits_n j_n e^{-E_n^{(0)}/kT}} . \tag{13}$$

Here, $E_n^{(0)}$ is the energy in zero field and N the Avogadro number. The quantities involved in Eq. (13) may be expressed according to

$$\begin{aligned} E_{nm}^{(1)} &= \langle \psi_{nm} | \sum_i \beta(\kappa l_{iz} + 2s_{iz}) H_z | \psi_{nm} \rangle \\ E_{nm}^{(2)} &= \sum_{n',m'} \frac{|\langle \psi_{nm} | \sum\limits_i \beta(\kappa l_{iz} + 2s_{iz}) H_z | \psi_{n'm'} \rangle|^2}{E_n^{(0)} - E_{n'}^{(0)}}, \quad n \neq n' . \end{aligned} \tag{14}$$

Here, the eigenvectors $|\beta \Gamma_T \gamma_T\rangle$, cf. Eq. (9), have been abbreviated by ψ_{nm} or $\psi_{n'm'}$. The matrix elements in Eq. (14) are thus identical to those of Eq. (11). However, we will show below that a considerable number of these matrix elements is, in fact, zero.

The eigenvectors $|\beta \Gamma_T \gamma_T\rangle$ may be classified within the group O_h by their behavior under the rotations C_4^z and C_4^x about the z- and the x-axis, respectively, according to the standard basis relations of Griffith [10]. The operator $L_z + 2S_z$ transforms under rotation about the z-axis according to $T_1 0$. In order to be different from zero, the matrix elements Eq. (11) have to be totally symmetric. Therefore, the only non-zero matrix elements are those listed below:

$$\begin{aligned} &\langle \Gamma_1 a_1 | L_z + 2S_z | \Gamma_4 0 \rangle , \\ &\langle \Gamma_2 a_2 | L_z + 2S_z | \Gamma_5 0 \rangle , \\ &\langle \Gamma_3\ \theta\ | L_z + 2S_z | \Gamma_4 0 \rangle , \\ &\langle \Gamma_3\ \varepsilon\ | L_z + 2S_z | \Gamma_5 0 \rangle , \\ &\langle \Gamma_4 \pm 1 | L_z + 2S_z | \Gamma_4 \pm 1 \rangle , \\ &\langle \Gamma_4 \pm 1 | L_z + 2S_z | \Gamma_5 \mp 1 \rangle , \\ &\langle \Gamma_5 \pm 1 | L_z + 2S_z | \Gamma_5 \pm 1 \rangle . \end{aligned}$$

Employing Eq. (9) these matrix elements may be decomposed into those of the functions $|\alpha S \Gamma \beta \Gamma_T \gamma_T\rangle$, the subsequently required ones being listed in Appendix II.

Numerical Results

Fig. 4 shows calculated values of the magnetic moment μ_{eff} (in BM) as function of temperature and of the octahedral ligand field splitting parameter 10 Dq. It is

$$\mu_{\text{eff}}^2 = \frac{3kT}{N\beta^2}\chi_m \tag{15}$$

where χ_m is determined according to Eq. (13) and Eq. (14) and $(3k/N\beta^2)^{1/2} = 2.827$. In the calculations, we employed the Fe^{2+} free ion parameters $B = 917\ \text{cm}^{-1}$, $C = 4040\ \text{cm}^{-1}$, and $\zeta = 420\ \text{cm}^{-1}$. All levels having zero field energies $E_n^{(0)} \leqq 5000\ \text{cm}^{-1}$ were considered directly in the summation of Eq. (13). This comprises, at 10 Dq = *II*, e.g., all those levels which result from the terms $^5T_2(t_2^4(^3T_1)\,e^2(^3A_2))$ and $^1A_1(t_2^6)$. In the matrix elements required in Eq. (14), all components of the eigenvectors $|\beta\Gamma_T\gamma_T\rangle$ Eq. (9) were included which are associated with coefficients $C_j \geqq 0.033$ at any value of 10 Dq considered. In this way, the following terms have been taken into account explicitly in Eq. (14): $^5T_2(t_2^4(^3T_1)e^2(^3A_2))$, $^3T_1(t_2^5\,e)$, $^1T_1(t_2^4\,e^2)$, $^1T_1(t_2^5\,e)$, $^1A_1(t_2^6)$, $^1A_1(t_2^4(^1E)\,e^2(^1E))$, $^1A_1(t_2^4(^1A_1)\,e^2(^1A_1))$. We checked that extending the range of terms considered to $E_n^{(0)} \leqq 8000\ \text{cm}^{-1}$ affected calculated values of μ_{eff} in the fifth decimal place at most.

In Fig. 5, similar plots of μ_{eff} vs. T and vs. 10 Dq are displayed for parameter values appropriate to the iron(II)poly(1-pyrazolyl)borate termed "compound I" of Jesson *et al.* [14], i.e. $B = 765\ \text{cm}^{-1}$, $C = 4.0$ B, $\zeta = 420\ \text{cm}^{-1}$, and $\kappa = 0.80$. In addition, the plot of experimental μ_{eff}-values vs. T for this compound has been included. In order to calculate μ_{eff}, the original molar susceptibility data [15] have been corrected by subtracting -0.29×10^{-3} cgs/mole [14]. From these results, values of 10 Dq and ε at various temperatures may be determined and these have been plotted in Fig. 6.

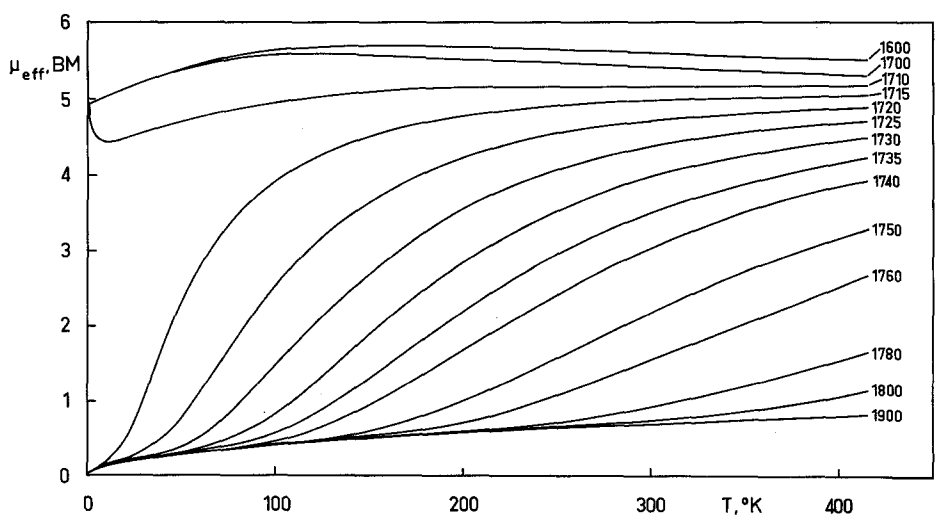

Fig. 4. Magnetic moment μ_{eff} of a d^6 ion in a field of octahedral symmetry versus temperature and 10 Dq ($B = 917\ \text{cm}^{-1}$, $C = 4040\ \text{cm}^{-1}$, $\zeta = 420\ \text{cm}^{-1}$, $\kappa = 1.0$)

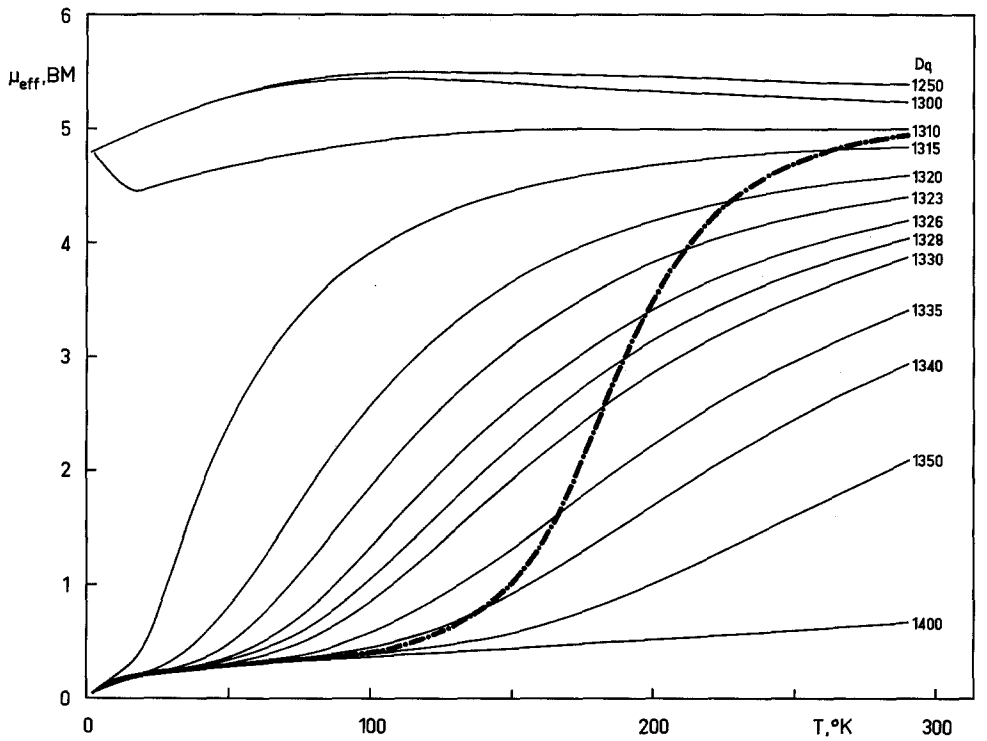

Fig. 5. Magnetic moment μ_{eff} of a d^6 ion in a field of octahedral symmetry versus temperature and 10 Dq ($B = 765$ cm^{-1}, $C = 4.0\ B$, $\zeta = 420$ cm^{-1}, $\kappa = 0.80$), full lines. Experimental μ_{eff}-values of the iron(II) poly(1-pyrazolyl)borate "compound I" of Jesson *et. al.* [14], broken line

Discussion and Conclusions

In general, in the calculation of paramagnetic susceptibilities, previous authors [16–19] have taken into account the ground state multiplet only and, in some special situations, the contribution of at most two of the lowest energy terms has been considered [20–22]. The only more detailed study [23] is concerned with the $^6A_1 - {}^2T_2$ crossover in d^5 ions and considers altogether three terms in approximate form. We are going to demonstrate below that, at least in the octahedral d^6 configuration, a small but definite influence of higher energy terms is evident.

The results of Fig. 4 show that, at low values of the ligand field parameter 10 Dq, e.g. at 10 Dq = 16,000 cm^{-1}, the calculated temperature dependence of μ_{eff} corresponds reasonably to the values determined from the $^5T_2(t_2^4\, e^2)$ multiplet alone [17, 19]. A more detailed comparison of the numerical data reveals small differences, however. Thus, at 400° K, e.g., we obtain $\mu_{eff} = 5.530$ BM whereas, if the $^5T_2$ term is considered alone, $\mu_{eff} = 5.564$ BM. These differences are subject to the mixing-in of excited state wavefunctions via spin-orbit interaction which is dependent on 10 Dq. Between 10 Dq = 16,800 cm^{-1} and 17,100 cm^{-1}, a decrease of μ_{eff} is observed as consequence of the mixing of the $\Gamma_1[^5T_2(t_2^4(^3T_1)\, e^2(^3A_2))]$ and $\Gamma_1[^1A_1(t_2^6)]$ states (at 10 Dq = 16,900 cm^{-1}, e.g., the Γ_1 state at 529.5 cm^{-1} consists

of 61.72% $|^5T_2(t_2^4(^3T_1)\,e^2(^3A_2))\rangle$, 36.72% $|^1A_1(t_2^6)\rangle$ and 1.56% various other contributions, whereas the Γ_1 state at 325.6 cm^{-1} is 57.42% $|^1A_1(t_2^6)\rangle$, 37.09% $|^5T_2(t_2^4(^3T_1)\,e^2(^3A_2))\rangle$, and 5.49% other contributions), cf. Fig. 3. At 10 Dq = 17,100 cm^{-1}, the $\Gamma_1[^1A_1(t_2^6)]$ state is still 1.44 cm^{-1} higher than the $\Gamma_1[^5T_2(t_2^4e^2)]$ state giving rise to the unusual change of μ_{eff} below 10° K. Above 10 Dq = 17,100 cm^{-1}, the typical crossover behavior sets in. In the high-temperature limit, almost all moment values between about 1.0 BM and 5.0 BM may be attained depending on 10 Dq, whereas, at the lowest temperatures, the resulting μ_{eff}-values are practically identical to those of a $^1A_1(t_2^6)$ term. In this region of 10 Dq values, the μ_{eff} vs. T curves are significantly different from those obtained on the basis of a simple two-level scheme [20]. The largest discrepancy arises with the magnetism of the $^1A_1(t_2^6)$ term both in the primitive $^5T_2 - {}^1A_1$ crossover model as well as at high values of 10 Dq ("low-spin" compounds), e.g., at and above 10 Dq = 17,500 cm^{-1}.

The magnetism of the $^1A_1(t_2^6)$ term deserves additional comments. This case has been treated separately by Griffith [10] and more recently by Sinn [24] without paying due regard to the effects of *complete* configuration interaction and spin-orbit coupling. Consequently, only order of magnitude results for μ_{eff} were obtained, *viz.* 0.8 to 0.9 BM at room temperature [24]. Of course, there is no first order interaction with the magnetic field in a pure $|^1A_1(t_2^6)\rangle$ state, since

$$\langle {}^1A_1(t_2^6)|\sum_i \beta(\kappa l_{iz} + 2s_{iz})H_z|\,{}^1A_1(t_2^6)\rangle = 0\,. \tag{16}$$

Therefore, all of the observed magnetic susceptibility in low-spin iron(II) compounds arises from mixing with higher states $|\alpha S\Gamma M\gamma\rangle$ via spin-orbit coupling or from interactions with these states through the Zeeman operator $\sum_i \beta(\kappa l_{iz} + 2s_{iz})H_z$. The eigenvector $|\Gamma_1[^1A_1(t_2^6)]\rangle$ is composed largely of the $|^1A_1(t_2^6)\rangle$ state, at least for high values of 10 Dq. Thus, e.g., at 10 Dq = 17,500 cm^{-1}, and with values of B, C, and ζ as employed above, this level consists of 93.80% $|^1A_1(t_2^6)\rangle$, 3.29% $|^1A_1(t_2^4(^1A_1)\,e^2(^1A_1))\rangle$, 2.02% $|^3T_1(t_2^5\,e)\rangle$, and 0.89% of other states. Due to the high magnetic moments, the contribution of states with spin multiplicities of 3 or 5, cf. $|^3T_1(t_2^5\,e)\rangle$, is not negligible. However, there is a second more important contribution to consider. As far as the $|^1A_1(t_2^6)\rangle$ state is concerned, the application of $\sum_i s_{iz}$ gives zero and thus any direct magnetic interaction must be through $\sum_i l_{iz}$. Now l_z transforms as T_10 and consequently the only non-zero magnetic interaction will be with $^1T_1$ states as shown above. The resulting behavior of μ_{eff} may be seen from Fig. 4. In contrast to the previous treatments [10, 24], there is a marked temperature dependence of the moment. Thus, if 10 Dq = 19,000 cm^{-1} is assumed, e.g., the moment decreases from $\mu_{eff} = 0.806$ BM at 400° K to 0.285 BM at 50° K and assumes even smaller values at lower temperatures. If 17,150 cm^{-1} < 10 Dq < 19,000 cm^{-1}, μ_{eff} is considerably larger in the high temperature limit than in the above example, however, it decreases with decreasing temperature and arrives in the low temperature limit at the same μ_{eff}-values as above.

The results of the present calculations are also of interest with respect to the intermediate magnetic moments observed in several iron(II) bis(diimine) complexes [25, 26]. Thus in $[Fe(phen)_2ox]\cdot 5H_2O$ (phen = 1,10-phenanthroline, ox = oxalate), e.g., the magnetic moment decreases from $\mu_{eff} = 4.32$ BM at 399.4° K

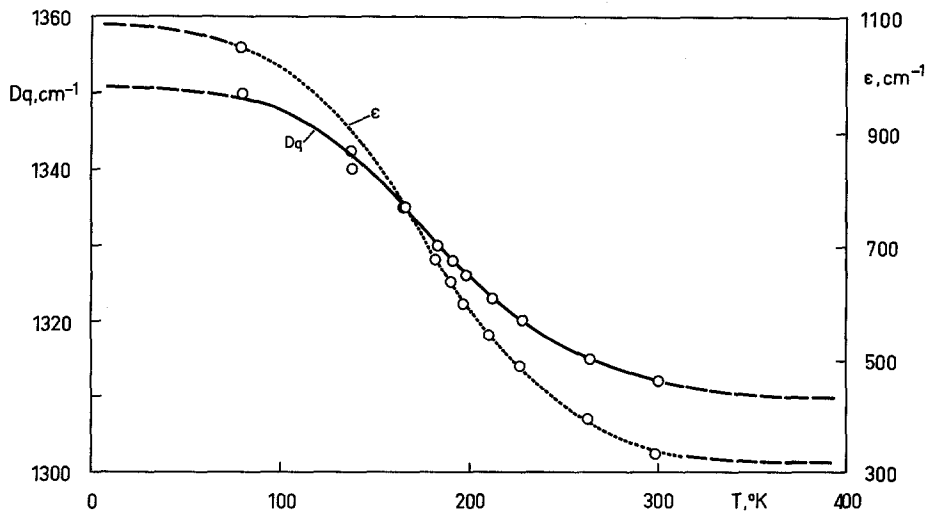

Fig. 6. 10 Dq and ε as function of temperature for the iron(II) poly(1-pyrazol)borate "compound I". Broken lines are extrapolated

to 3.69 BM at 76.8° K according to the Curie-Weiss law with $\Theta = -20°$. Comparable results are obtained for a series of similar compounds. It follows that the observed magnetism does not fit into the family of curves of Fig. 4 since, in that case, much smaller μ_{eff}-values would be expected at the lowest temperature studied. The magnetism of these compounds thus cannot be explained on the basis of a ${}^1A_1(t_2^6)$ ground state and a thermally accesible ${}^5T_2(t_2^4 e^2)$ state, at least not under the assumption of octahedral symmetry.

The iron(II) poly(1-pyrazolyl)borate called "compound I", the magnetism of which is compared with the results of our calculations in Fig. 5, has been shown to exhibit a ${}^5T_2 - {}^1A_1$ equilibrium between $\sim 260°$ and $\sim 160°$ K [14]. The experimental curve of μ_{eff} vs. T is not expected to conform to any of the calculated curves in Fig. 5 since, during the transition, 10 Dq should change from a lower value characteristic of the ${}^5T_2$ ground state to a higher value characteristic of the ${}^1A_1$ state or vice versa [4]. From the points of intersection of the experimental and the calculated curves, 10 Dq may be determined at a number of temperatures, *viz.* Fig. 6. According to this graph, 10 Dq shows indeed the expected variation with temperature. In addition, values of ε were determined analogously and these are included in Fig. 6. In contrast to the results of a semi-empirical analysis of experimental data [1], the variation of ε with temperature observed here should be valid in general. We would like to point out, however, that quantitative results cannot be expected since, in the compound studied, we have disregarded an axial field splitting corresponding to $\delta = -1000\ \text{cm}^{-1}$ [14]. Nonetheless we believe that the example is instructive as it stands.

The present investigation thus demonstrates, on the particularly involved d^6 problem, that a complete calculation of the magnetic susceptibility is both feasible and rewarding.

Appendix I

Below we present detailed expressions for the eigenvectors $|\beta\Gamma_T\gamma_T\rangle$ resulting from the lowest energy terms $^5T_2$, $^1A_1$, and $^3T_1$ at 10 Dq $= \Pi = 17{,}100$ cm^{-1} on application of spin-orbit coupling. Only coefficients larger than 0.100 have been included.

$$|\Gamma_1[^1A_1(t_2^6)]\rangle = 0.946|^1A_1(t_2^6)\rangle + 0.208|^5T_2(t_2^4(^3T_1)\,e^2(^3A_2))\rangle - 0.179|^1A_1(t_2^4(^1A_1)\,e^2(^1A_1))\rangle - 0.160|^3T_1(t_2^5\,e)\rangle$$

$$|\Gamma_1[^5T_2(t_2^4(^3T_1)\,e^2(^3A_2))]\rangle = 0.972|^5T_2(t_2^4(^3T_1)\,e^2(^3A_2))\rangle - 0.217|^1A_1(t_2^6)\rangle$$

$$|\Gamma_3[^5T_2(t_2^4(^3T_1)\,e^2(^3A_2))]\rangle = 0.997|^5T_2(t_2^4(^3T_1)\,e^2(^3A_2))\rangle$$

$$|2\Gamma_4[^5T_2(t_2^4(^3T_1)\,e^2(^3A_2))]\rangle = 0.994|^5T_2(t_2^4(^3T_1)\,e^2(^3A_2))\rangle$$

$$|3\Gamma_4[^5T_2'(t_2^4(^3T_1)\,e^2(^3A_2))]\rangle = 0.991|^5T_2'(t_2^4(^3T_1)\,e^2(^3A_2))\rangle$$

$$|1\Gamma_5[^5T_2(t_2^4(^3T_1)\,e^2(^3A_2))]\rangle = 0.999|^5T_2(t_2^4(^3T_1)\,e^2(^3A_2))\rangle$$

$$|3\Gamma_5[^5T_2'(t_2^4(^3T_1)\,e^2(^3A_2))]\rangle = 0.997|^5T_2'(t_2^4(^3T_1)\,e^2(^3A_2))\rangle$$

$$|\Gamma_1[^3T_1(t_2^5\,e)]\rangle = 0.966|^3T_1(t_2^5\,e)\rangle + 0.139|^1A_1(t_2^6)\rangle + 0.127|^3T_1(t_2^3(^2T_2)\,e^3)\rangle + 0.106|^5T_2(t_2^4(^3T_1)\,e^2(^3A_2))\rangle + 0.101|^3T_1(t_2^4(^3T_1)\,e^2(^1A_1))\rangle$$

$$|\Gamma_3[^3T_1(t_2^5\,e)]\rangle = 0.976|^3T_1(t_2^5\,e)\rangle - 0.135|^3T_1(t_2^4(^3T_1)\,e^2(^1E))\rangle + 0.116|^3T_1(t_2^2\,e^4)\rangle$$

$$|\Gamma_4[^3T_1(t_2^5\,e)]\rangle = 0.976|^3T_1(t_2^5\,e)\rangle + 0.125|^3T_1(t_2^3(^2T_2)\,e^3)\rangle - 0.105|^3T_1(t_2^4(^3T_1)\,e^2(^1E))\rangle$$

$$|\Gamma_5[^3T_1(t_2^5\,e)]\rangle = 0.976|^3T_1(t_2^5\,e)\rangle - 0.135|^3T_1(t_2^4(^3T_1)\,e^2(^1E))\rangle + 0.116|^3T_1(t_2^2(^3T_1)\,e^4)\rangle\,.$$

Concerning the first label in the Γ_4 and Γ_5 kets above, Appendix II should be consulted.

Appendix II

The construction of the wavefunctions $|\alpha S\Gamma M\gamma\rangle$ was effected according to procedures described by Griffith [10] making extensive use of the Tables A20 and A24. The subsequent coupling of spin and orbital states employed Table A19 in addition and was accomplished similarly. This procedure yields basis functions $|\alpha S\Gamma\beta\Gamma_T\gamma_T\rangle$ four of which are different from those implicitly assumed by Schroeder [12]. It is the functions which were denoted by Schroeder as $|\Gamma_5[^5T_2(t_2^4(^3T_1)\,e^2(^3A_2))]\rangle$ and $|\Gamma_4[^5T_2(t_2^4(^3T_1)\,e^2(^3A_2))]\rangle$, primed and unprimed. In addition, it should be observed that there are differences in phase between our functions and those of Schroeder. Both approaches arrive, however, at the same eigenvalues of the spin-orbit coupling operator.

Below we list the matrix elements

$$\langle\alpha S\Gamma\beta\Gamma_T\gamma_T|\sum_i \beta(\kappa l_{iz} + 2s_{iz})H_z|\alpha' S'\Gamma'\beta'\Gamma_T'\gamma_T'\rangle\,,$$

which are different from zero. In the functions $|\alpha S \Gamma \beta \Gamma_T \gamma_T\rangle$, we use the standard notation of Griffith. Particularly, to differentiate between the two $|\Gamma_5{}^5T_2\rangle$ and the two $|\Gamma_4{}^5T_2\rangle$ functions mentioned above, we employ the quantum number $J=1,2,3$ which is based on the p^n isomorphism (cf. Table A20 of [10]). This quantum number is equivalent to the label β used in the functions $|\alpha S \Gamma \beta \Gamma_T \gamma_T\rangle$. For convenience of notation we introduce the following abbreviations:

$$
\begin{aligned}
&|{}^1A_1(t_2^6)\rangle = a\\
&|{}^1A_1(t_2^4({}^1E)\, e^2({}^1E))\rangle = b\\
&|{}^1A_1(t_2^4({}^1A_1)\, e^2({}^1A_1))\rangle = c\\
&|{}^1T_1(t_2^5\, e)\rangle = d\\
&|{}^1T_1(t_2^4\, e^2)\rangle = e\\
&|{}^3T_1(t_2^5\, e)\rangle = f\\
&|{}^5T_2(t_2^4({}^3T_1)\, e^2({}^3A_2))\rangle = g\,.
\end{aligned}
$$

The required matrix elements of the operator $\sum_i \beta(\kappa l_{iz} + 2s_{iz})H_z$ may then be written as stated in the compilation below. For simplicity, the operator has not been written explicitly. In addition, all matrix elements should be multiplied by βH.

$$
\begin{aligned}
\langle \Gamma_1 a \,||\, \Gamma_4 0 d\rangle &= +\,2\sqrt{2}\kappa\\
\langle \Gamma_1 f \,||\, \Gamma_4 0 f\rangle &= \frac{1}{\sqrt{6}}(4-\kappa)\\
\langle \Gamma_1 b \,||\, \Gamma_4 0 d\rangle &= -\frac{2}{\sqrt{3}}\kappa\\
\langle \Gamma_1 c \,||\, \Gamma_4 0 d\rangle &= -\frac{2}{\sqrt{3}}\kappa\\
\langle \Gamma_1 b \,||\, \Gamma_4 0 e\rangle &= -\sqrt{2}\kappa\\
\langle \Gamma_1 g \,||\, \Gamma_4 02 g\rangle &= \frac{\sqrt{2}}{3}(2+\kappa)\\
\langle \Gamma_1 g \,||\, \Gamma_4 03 g\rangle &= \frac{2}{3}(4-\kappa)\\
\langle \Gamma_3 \theta f \,||\, \Gamma_4 0 f\rangle &= \frac{1}{2\sqrt{3}}(4-\kappa)\\
\langle \Gamma_3 \theta g \,||\, \Gamma_4 02 g\rangle &= \frac{1}{3}(10-\kappa)\\
\langle \Gamma_3 \theta g \,||\, \Gamma_4 03 g\rangle &= \frac{\sqrt{2}}{3}(2+\kappa)\\
\langle \Gamma_3 \varepsilon f \,||\, \Gamma_5 0 f\rangle &= \frac{1}{2}(4+\kappa)
\end{aligned}
$$

$$\langle \Gamma_3 \varepsilon g || \Gamma_5 03 g \rangle = -\frac{\sqrt{2}}{\sqrt{5}}(2+\kappa)$$

$$\langle \Gamma_3 \varepsilon g || \Gamma_5 01 g \rangle = -\frac{\sqrt{3}}{\sqrt{5}}(2+\kappa)$$

$$\langle \Gamma_4 \pm 1 f || \Gamma_4 \pm 1 f \rangle = \pm\frac{1}{4}(4-\kappa)$$

$$\langle \Gamma_4 \pm 13 g || \Gamma_4 \pm 13 g \rangle = \pm\frac{1}{6}(4-\kappa)$$

$$\langle \Gamma_4 \pm 13 g || \Gamma_4 \pm 12 g \rangle = \pm\frac{\sqrt{2}}{3}(2+\kappa)$$

$$\langle \Gamma_4 \pm 12 g || \Gamma_4 \pm 12 g \rangle = \mp\frac{1}{6}(10-\kappa)$$

$$\langle \Gamma_4 \pm 1 f || \Gamma_5 \mp 1 f \rangle = \mp\frac{1}{4}(4-\kappa)$$

$$\langle \Gamma_4 \pm 13 g || \Gamma_5 \mp 13 g \rangle = \pm\frac{\sqrt{15}}{6}(4-\kappa)$$

$$\langle \Gamma_4 \pm 12 g || \Gamma_5 \mp 11 g \rangle = \pm\frac{3}{2\sqrt{5}}(2+\kappa)$$

$$\langle \Gamma_4 \pm 12 g || \Gamma_5 \mp 13 g \rangle = \mp\frac{2}{\sqrt{30}}(2+\kappa)$$

$$\langle \Gamma_5 \pm 1 f || \Gamma_5 \pm 1 f \rangle = \mp\frac{1}{4}(4+\kappa)$$

$$\langle \Gamma_5 \pm 11 g || \Gamma_5 \pm 1 g \rangle = \pm\frac{1}{2}(6+\kappa)$$

$$\langle \Gamma_5 \pm 13 g || \Gamma_5 \pm 3 g \rangle = \mp\frac{1}{2}(4-\kappa)\,.$$

Acknowledgements. The authors appreciate financial support by the Deutsche Forschungsgemeinschaft, the Fonds der Chemischen Industrie, and the Stiftung Volkswagenwerk. The communication of experimental magnetic data by Dr. F. Weiher, Wilmington, Del., is also gratefully acknowledged.

References

1. König, E., Kremer, S.: Theoret. chim. Acta (Berl.) **20**, 143 (1971).
2. Van Santen, J.H., Van Wieringen, J.S.: Recueil Trav. chim. Pays-Bas **71**, 420 (1952).
3. König, E., Watson, K.J.: Chem. Physics Letters **6**, 457 (1970).
4. — Kremer, S.: Chem. Physics Letters **8**, 312 (1971).
5. — Ritter, G., Spiering, H., Kremer, S., Madeja, K., Rosenkranz, A.: J. chem. Physics in the press.
6. — — Goodwin, H.A.: to be published.
7. Tanabe, Y., Sugano, S.: J. Physic. Soc. Japan **9**, 753 (1954).
8. — — J. Physic. Soc. Japan **9**, 766 (1954).
9. Jørgensen, C.K.: Advances chem. Physics **5**, 33 (1963).

10. Griffith, J.S.: The theory of transition metal ions. Cambridge: University Press 1961.
11. König, E., Kremer, S.: to be published.
12. Schroeder, K.A.: J. chem. Physics **37**, 2553 (1962).
13. Van Vleck, J.H.: The theory of electric and magnetic susceptibilities. Oxford: University Press 1932.
14. Jesson, J.P., Weiher, J.F., Trofimenko, S.: J. chem. Physics **48**, 2058 (1968).
15. Weiher, J.F.: Personal communication.
16. Kotani, M.: J. Physic. Soc. Japan **4**, 293 (1949).
17. Griffith, J.S.: Trans. Faraday Soc. **54**, 1109 (1958).
18. Figgis, B.N.: Nature **182**, 1568 (1958).
19. König, E., Chakravarty, A.S.: Theoret. chim. Acta (Berl.) **9**, 151 (1967).
— — Madeja, K.: Theoret. chim. Acta (Berl.) **9**, 171 (1967).
20. — Madeja, K.: Inorg. Chem. **6**, 48 (1967); Inorg. Chem. **7**, 2677 (1968).
21. Ewald, A.H., Martin, R.L., Ross, I.G., White, A.H.: Proc. Roy. Soc. (London) A **280**, 235 (1964).
22. Barraclough, C.G.: Trans. Faraday Soc. **62**, 1033 (1966).
23. De Lisle, J.M., Golding, R.M.: Proc. Roy. Soc. (London) A **296**, 457 (1967).
24. Sinn, E.: Inorg. Chim. Acta **3**, 11 (1969).
25. König, E., Madeja, K.: J. Amer. chem. Soc. **88**, 4528 (1966).
26. — — Inorg. Chem. **7**, 1848 (1968).

Dozent Dr. E. König
Institut für Physikalische Chemie II
Fahrstraße 17
BRD-8520 Erlangen, Germany